Advances in Robotics & Automation

Wang and Artemiadis, Adv Robot Autom 2013, 2:3
DOI: 10.4172/2168-9695.1000110

Research Article Open Access

Closed-Form Inverse Kinematic Solution for Anthropomorphic Motion in Redundant Robot Arms

Yuting Wang and Panagiotis Artemiadis*

Mechanical and Aerospace Engineering, School for Engineering of Matter, Transport and Energy, Arizona State University Tempe, USA

Abstract

As robots are increasingly migrating out of factories and research laboratories and into our everyday lives, they should move and act in environments designed for humans. For this reason, the need of anthropomorphic movements is of utmost importance. This paper proposes a framework for solving the inverse kinematics problem of redundant robot arms that results to anthropomorphic configurations. The swivel angle of the elbow is used as a human arm motion parameter for the robot arm to mimic. The swivel angle is defined as the rotation angle of the plane defined by the upper and lower arm around a virtual axis that connects the shoulder and wrist joints. Using kinematic data recorded from human subjects during every-day life tasks, we validate the linear relations between intrinsic and extrinsic coordinates of the human arm that estimates the swivel angle, given the desired end-effector position. Defining the desired swivel angle simplifies the kinematic redundancy of the robot arm. The proposed method is tested with an anthropomorphic redundant robot arm and the computed motion profiles are compared to the ones of the human subjects. We show that the method computes anthropomorphic configurations for the robot arm, even if the robot arm has different link lengths than the human arm and starts its motion at random configurations.

Keywords: Human arm kinematics; Robot arm model; Redundancy resolution; Anthropomorphic motion

Introduction

During the last decade, robots have successfully migrated out of factories and academic labs and into our. Every day lives, creating new families of co-robots and bionics. These robots should be able to move and act in environments designed for humans, and more importantly use tools for executing tasks designed for humans. Therefore, there is an increasing demand of robots which can interact, communicate and collaborate with humans. This requires human-like behaviour, which will allow the human subject to be able to understand robot's intentions and seamlessly collaborate with the robot. Its application fields range widely from service robotics to therapeutic devices [1]. In order for the human-robot cooperation to be intuitive, the robot configurations should be anthropomorphic [2,3]. This is not straightforward, since the human arm is redundant, i.e. it has 7 degrees of freedom (DOFs), while only 6 DOFs are required for a given position and orientation of the arm endpoint. This creates a challenge for the redundant robot inverse kinematics that need to be solved in a similar way of that of the human arm, in order to guarantee seamless integration [4-6]. The exploitation of kinematic redundancy for the generation of human-like robot arm motions has been already proposed in the literature. In Cruse [7], it is shown that it is possible to associate some cost function to each human arm joint. The arm performs movements that optimize these cost functions. A variety of cost functions have been used to explain the principles of human arm motor control, such as ones related to dynamics [8-10], neuro-physiological and psychophysical ones [11-13], as well as combinations of those [7,14]. However, the majority of these cost functions are used with global optimization methods which are computationally expensive and not suitable for real-time implementation. In [3,15], a mathematical cost functional describing the muscle fatigue is used to achieve human-like joint motions of a robot arm during writing tasks. Even though it is of a local nature, the applicability of this method to generate human-like manipulation motions is not yet clear. Human motion capture has been widely used for the generation of kinematic models describing human and humanoid robot motions [16]. There have been also efforts to generate human-like motion by imitating human arm motion as closely as possible. In Kim [17], a method to convert the captured marker data of human arm motions to robot motion using an optimization scheme is proposed. The position and orientation of the human hand, along with the orientation of the upper arm, were imitated by a humanoid robot arm.

However, this method was not able to generate human-like motions, given a desired three dimensional (3D) position for the robot end-effector. Similarly, most of the previous works on biomimetic motion generation for robots are based on minimizing posture difference between the robot and human arm, using a specific recorded data set [18,19]. Therefore, the robot configurations are exclusively based on the recorded data set. In this way, the methods can not generate new human-like motion. The latter is a major limitation for the kinematic control of anthropomorphic robot arms and humanoids, because the range of possible configurations is limited to the ones seen in the data. In [4], a method is proposed to solve the inverse kinematic problem by defining the swivel angle, i.e. the rotation angle of the plane defined by the upper and lower arm around a virtual axis that connects the shoulder and wrist joints. However, the method is only demonstrated for simple tasks, i.e. natural reaching and grasping, while the method

***Corresponding author:** Panagiotis Artemiadis, Mechanical and Aerospace Engineering, School for Engineering of Matter, Transport and Energy, Arizona State University Tempe, USA, Tel: 480-965-4182; E-mail: panagiotis.artemiadis @asu.edu

Received November 04, 2013; **Accepted** December 04, 2013; **Published** December 06, 2013

Citation: Wang Y, Artemiadis P (2013) Closed-Form Inverse Kinematic Solution for Anthropomorphic Motion in Redundant Robot Arms. Adv Robot Autom 2: 110. doi: 10.4172/2168-9695.1000110

requires the initial configuration of the human arm and the robot arm to be known, a feature that is not readily available in real scenarios. In Asfour [2], the upper arm joints values are first calculated for positioning the robot elbow and then the remaining joints are solved with closed-form inverse kinematics. Such an approach though cannot be easily applied to robots having a kinematic structure different from that of the human upper limb. There are also some biomimetic approaches based on the dependencies among the human joint angles [1,20]. In Edsinger A [1], the authors generalized the inverse kinematic solution by encompassing joint limitation, singularity avoidance and optimum manipulability measures. However, the proposed requires the robot arm with similar structure of the human arm, while its iterative solution method is not efficient for real-time processing. In this paper we consider the problem of generating human-like motions from the kinematic point of view taking into account data recorded during a wide variety of everyday life tasks. We rely on a hypothesis from neurophysiology and apply it for generating human-like motions of a redundant anthropomorphic robot arm. The human arm swivel angle is used as a parameter for the robot arm to mimic, and the problem of the inverse kinematics is simplified. The linear relationship between the intrinsic and extrinsic coordinates was validated and used to estimate the desired swivel angle using previous knowledge of human arm motion recordings. The proposed controller is finally applied to a 7 DOFs robot arm (LWR 4+, KUKA) for evaluation purposes.

Method

Human arm kinematics

As it shown in Figure 1, the human arm consists of a series of rigid links connected by three anatomical joints (shoulder joint, elbow joint, and wrist joint) while neglecting the scapular and clavicle motions [21]. In this study, 7 DoFs were analyzed for simplicity: shoulder exion-extension, shoulder abduction-adduction, shoulder lateral-medial rotation, elbow exion-extension, elbow pronation-supination, wrist exion-extension and wrist pronation-supination, which can be simulated by 7 corresponding joint angles, i.e. q1, q2, q3, q4, q5, q6,q7 for the human arm. The Denavit-Hartenberg (DH) parameters of the kinematic model of the arm that we used are listed in Table 1 [1,20] where L1, L2, L3 are the lengths of the upper arm, forearm and palm respectively1. In order to track the motion of the upper limb, a 3D position sensor and associated positioning markers attached to each rigid link were used to compute the joint angles of the shoulder, elbow and wrist. The position and orientation of the end effector for the human arm can be expressed as a function of all those joint angles through forward kinematics.

Robot arm model

Figure 1 also shows the reference and link coordinate systems of the 7-DoF robot arm (LWR4+, KUKA) using the DH convention [22]. The values of the DH parameters are listed in Table 2, where Lu, Lf and Lh are the link lengths of robot upper-arm, forearm and hand respectively. There are several differences between the human arm and the robot arm:

1. The human arm has a spherical wrist (q5, q6 and q7 axes intersect at a single point) while the robot arm does not.
2. The length of the KUKA arm is almost twice as much as that of the human arm.

Reduction of number of joint variables

For a given position and orientation of the end-effector with respect to the base frame, the wrist position can be easily defined. As shown in Figure 2, once the end-effector position and orientation are specified in terms of p_{ee} and $R_{ee}=[n\ s\ a]$, so that the homogeneous transformation relating the description a point in the end-effector frame to the description of the same point in base frame can be represented as

$$T^{b}_{e}=\begin{bmatrix} n & s & a & p_{ee} \\ 0 & 0 & 0 & 1 \end{bmatrix} \quad (1)$$

then the wrist position in the end-effector frame can be represented as

$$P_{we}=\begin{bmatrix} d_x \\ d_y \\ d_z \end{bmatrix}=d \quad (2)$$

i	α_i	a_i	d_i	θ_i
1	90°	0	0	q_1
2	90°	0	0	q_2 + 90°
3	90°	0	L_1	q_3 + 90°
4	90°	0	0	q_4 + 180°
5	90°	0	L_2	q_5 + 180°
6	90°	0	0	q_6 + 90°
7	90°	L_3	0	q_7 + 180°

Table 1: Human arm D-H parameters.

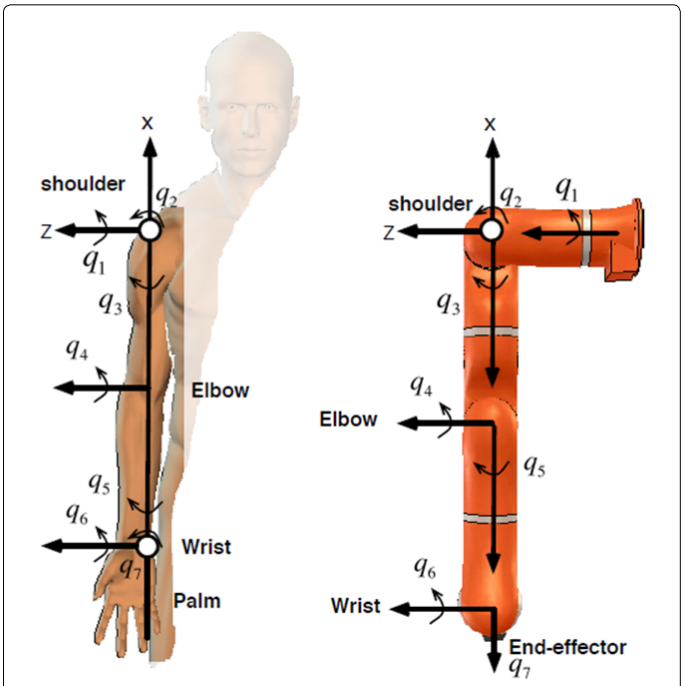

Figure 1: Kinematic models of the Human and Robot arms.

i	α_i	a_i	d_i	θ_i
1	90°	0	0	q_1
2	90°	0	0	q_2
3	90°	0	L_u	q_3
4	90°	0	0	q_4
5	90°	0	L_f	q_5
6	90°	0	0	q_6
7	0	0	L_h	q_7

Table 2: KUKA arm model D-H parameters.

Where dx, dy, dz are the coordinates of the wrist center with respect to the origin of the end-effector frame. This allows direct computation of the wrist position with respect to the base frame given the end-effector frame [22]. In our case, the base frame is located at the center of the shoulder for both arm models shown in Figure 1. Therefore, the position of the wrist Pw in the base frame can be found as:

$$\begin{bmatrix} P_w \\ 1 \end{bmatrix} = T^b_e \begin{bmatrix} P_{we} \\ 1 \end{bmatrix} \quad (3)$$

Therefore, given a desired position and orientation of the end-effector, we split the problem into two parts:

1. Using (3) we compute the wrist position, and since the wrist position is only a function of the first 4 joint angles (q1-q4) we define a method to solve for those joints. This step involves redundancy in joint angles and it is going to be solved in a way to guarantee anthropomorphism (see Redundancy resolution section).
2. Knowing q1-q4 and the desired position and orientation of the end-effector frame, we can then analytically solve for q5-q7. Therefore, we can neglect the structure difference of these two arms.

Redundancy resolution

There is evidence from previous works that the position of the elbow joint in space is an important parameter of anthropomorphism for arm configurations [4,2]. The redundancy of the arm is actually found on the first four joints, that need to position the wrist on a 3D position in Cartesian Space. A simple physical interpretation of the redundant degree of freedom is based on the observation that if the wrist is held fixed, the elbow is still free to swivel about a circular arc whose normal vector is parallel to the axis from the shoulder to the wrist [23]. In Veljko P (3), P_s, P_e and P_w represents the position of the shoulder, the elbow and the computed location of the wrist based on the given position and orientation of the end effector. As the swivel angle ϕ varies, the elbow traces an arc of a circle lying on a plane which is perpendicular to the wrist-to-shoulder axis. In order to measure ϕ, we define the normal vector of the plane as $\tilde{n}$, P_c as the center of the circle and unit vector $\tilde{u}$, $\tilde{v}$ as the coordinate system on the plane. Here $\tilde{u}$ is set as the projection of an arbitrary vector $\tilde{a}$ onto the plane and $\tilde{v}$ is the cross product of $\tilde{u}$ and $\tilde{n}$.

The selection of $\tilde{}$ will determine where $\phi = 0[23, 4]$. Therefore, the position of the elbow can be represented as:

$$P_e = R\left[\cos(\phi)\tilde{u} + \sin(\phi)\tilde{v}\right] + P_c \quad (4)$$

where R is the Euclidean distance between P_e and P_c.

The analytic expression above is an advantage when an objective function is used to select an appropriate value of ϕ since it is often necessary to express the objective function in terms of the joint angles. Once the value of ϕ is determined, the elbow position can be computed. With the position of the wrist and elbow, as well at the 3D position and orientation of the rigid body of the end effector, we are able to analytically give a unique solution to the inverse kinematic problem, and therefore compute the 7 joint angles of the upper limb.

Another benefit of the swivel angle is that it is not constrained by the limitation of the arm length. In Hyunchul [4], it has been proven that the direction of the longest axis in the manipulability ellipsoid of the wrist is only a function of the swivel angle. Therefore, the swivel angle of the robot arm should be selected close to that of the human arm with the same position and orientation of the end effector in order to maintain the manipulability which leads to an anthropomorphic configuration. This will be validated in the Results section.

The linear relationships between intrinsic and extrinsic coordinates

The idea to generate anthropomorphic robot arm motions is inspired by the results obtained in [24,25]. The arm movements are in shoulder-centered spherical coordinates and there is a linear sensorimotor transformation model that maps the extrinsic coordinates on a natural arm posture using the intrinsic coordinates. The extrinsic coordinates are the wrist position expressed in the spherical coordinates, where R denotes the radial distance, χ the azimuth, and ψ the elevation. The reason to choose the spherical coordinates rather than Cartesian or cylindrical is the former leads to a more compact representation of the linear relation [24]. The wrist position in the Cartesian coordinates can be transformed to the spherical coordinates by:

$$R2 = P_w(x)^2 + P_w(y)^2 + P_w(x)^2 \quad (5)$$

$$\tan(\chi) = \frac{P_w(z)}{-P_w(y)} \quad (6)$$

$$\tan(\varphi) = \frac{P_w(x)}{\sqrt{P_w(y)^2 + P_w(z)^2}} \quad (7)$$

Where $P_w(x), P_w(y)$ *and* $P_w(z)$ designate the Cartesian components of the wrist position with respect to the shoulder frame. The intrinsic coordinates consist of angles defined the upper arm elevation (θ) and yaw (η) and the forearm elevation (α) and yaw (β). The elevations (θ, β) define the angle between each limb segment and the vertical axis measured in a vertical plane. The yaw angles (η, α) define the angle between each of the limb segments and the anterior direction, measured in the horizontal plane, as shown in Figure 3. However, this linear relation has only been proven by one simple task, arm pointing in [24,25]. Here, we demonstrate a more accurate relationship with more daily life tasks (see Results section).

Based on this linear relationship, the orientation angles of the upper arm and the forearm $(\theta, \eta, \alpha, \beta)$ can be obtained only knowing the wrist position (R, χ, φ). Therefore, as is shown in Figure 4, the elbow position in this coordinate system can be expressed as:

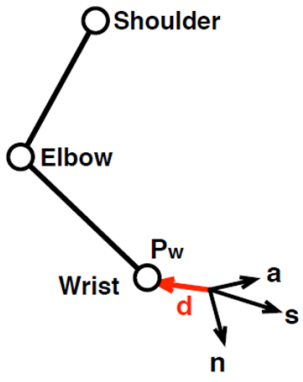

Figure 2: Wrist position with respect to the end-effector frame.

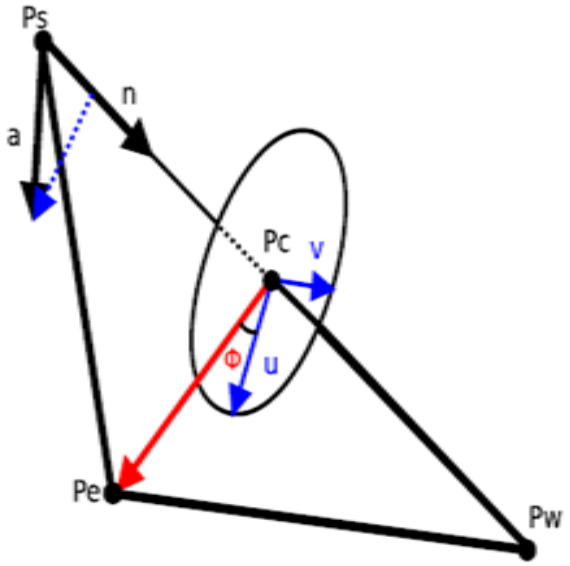

Figure 3: Coordinate frame at the center of the elbow circle and the swivel angle that allows the parameterization of the elbow position by a single variable.

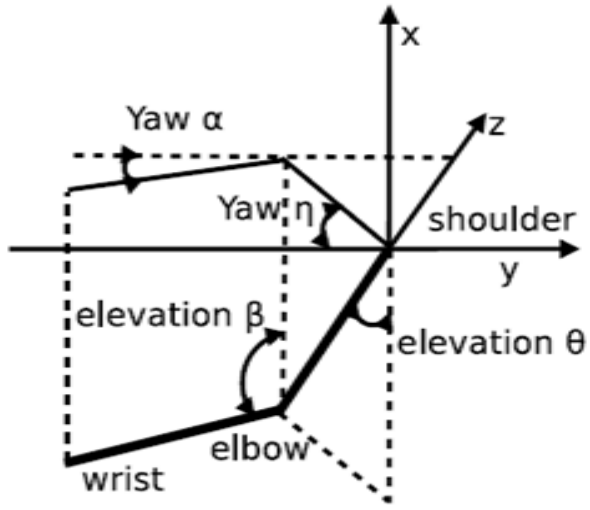

Figure 4: Orientation angles of the arm and forearm. The angles θ and η define the elevation and the yaw of the upper arm and β and α represent the elevation and yaw of the forearm.

$$P_e(x) = -U\cos(\theta) \tag{8}$$

$$P_e(y) = -U\sin(\theta)\cos(\eta) \tag{9}$$

$$P_e(z) = U\sin(\theta)\sin(\eta) \tag{10}$$

Where $P_e(x), P_e(y)$ *and* $P_e(z)$ designate the components of the elbow position with respect to the shoulder frame. U represents the length of the upper arm.

The swivel angle can be obtained knowing the elbow position computed by (8,9,10) and wrist position computed by (3). Then the swivel angle is selected using (4):

$$\phi = a\tan 2\left(\frac{(P_e - P_c).\vec{u}}{\|P_e - P_c\|}, \frac{(P_e - P_c).\vec{v}}{\|P_e - P_c\|}\right) \tag{11}$$

Solution for inverse kinematic problem

Let $P_e = [x_e \;\; y_e \;\; z_e]^T$, $P_w = [x_w \;\; y_w \;\; z_w]^T$ be the position of the elbow and wrist with respect to the base frame. The position of the elbow is computed by (4), with the estimation of the swivel angle, using (11). The position of the wrist is computed using (3). Let the desired position and orientation of the end- effector be given by

$$T = \begin{bmatrix} n_d & s_d & a_d & p_d \\ 0 & 0 & 0 & 1 \end{bmatrix} \tag{12}$$

Since the position of the wrist and elbow are computed, then the solution for the first 4 joint angles has a

closed form which is shown below:

$$q_1 = \arctan 2(y_e, x_e) \tag{13}$$

$$q_2 = \arctan 2\left(\sqrt{(x_e)^2 + (y_e)^2}, z_e\right) \tag{14}$$

$$q_3 = \arctan 2(-M_3, M_1) \tag{15}$$

$$q_4 = \arctan 2\left(\sqrt{(M_1)^2 + (M_3)^2}, M_2 - L_1\right) \tag{16}$$

Where

$$M_1 = x_w\cos(q_1)\cos(q_2) + y_w\sin(q_1)\cos(q_2) z_w\sin(q_2) \tag{17}$$

$$M_2 = x_w\cos(q_1)\sin(q_2) y_w\sin(q_1)\sin(q_2) z_w\cos(q_2) \tag{18}$$

$$M_3 = x_w\sin(q_1) + y_w\cos(q_2) \tag{19}$$

We should note that although multiple solutions could arise, they are eliminated by violating the human

joint limitations. In order to solve for q5-q7, we can articulate the inverse kinematics problem into two sub-problems. After solving the inverse kinematics for q1 to q4, we can compute the transformation matrix from the base frame to the wrist frame, ${T^0}_4(q_1, q_2, q_3, q_4)$. Then, the transformation matrix from the wrist frame to the end-effector frame can be computed as

$${T^4}_7(q_5, q_6, q_7) = \begin{bmatrix} n_x^{(4)} & s_x^{(4)} & a_x^{(4)} & p_x^{(4)} \\ n_y^{(4)} & s_y^{(4)} & a_y^{(4)} & p_y^{(4)} \\ n_z^{(4)} & s_z^{(4)} & a_z^{(4)} & p_z^{(4)} \\ 0 & 0 & 0 & 1 \end{bmatrix} = (T^0{}_4)^T T \tag{20}$$

Where

$$n^{(4)} = \begin{bmatrix} n_x^{(4)} & n_y^{(4)} & n_z^{(4)} \end{bmatrix}^T, s^{(4)} = \begin{bmatrix} s_x^{(4)} & s_y^{(4)} & s_z^{(4)} \end{bmatrix}^T, a^{(4)} = \begin{bmatrix} a_x^{(4)} & a_y^{(4)} & a_z^{(4)} \end{bmatrix}^T$$

are the orientation vectors and $p^{(4)} = \begin{bmatrix} p_x^{(4)} & p_y^{(4)} & p_z^{(4)} \end{bmatrix}^T$ is the position vector of the end-effector reference system with respect to the one at the wrist. Since ${T^4}_7(q_5, q_6, q_7)$ is known, the joint angles q_5, q_6, q_7 can be computed using (20). The analytical solution is given by:

$$q_5 = \arctan 2(a_y^{(4)}, a_x^{(4)}) \tag{21}$$

$$q_6 = \arctan 2\left(\sqrt{(a_y^{(4)})^2 + (a_x^{(4)})^2}, a_z^{(4)}\right) \tag{22}$$

$$q_7 = \arctan 2(n_z^{(4)}, -s_z^{(4)}) \tag{23}$$

For $q_5 \varepsilon (0, \pi)$

$$q_5 = \arctan 2(-a_y^{(4)}, -a_x^{(4)}) \quad (24)$$

$$q_6 = \arctan 2\left(-\sqrt{(a_y^{(4)})^2 + (a_x^{(4)})^2}, a_z^{(4)}\right) \quad (25)$$

$$q_7 = \arctan 2(-n_z^{(4)}, s_z^{(4)}) \quad (26)$$

For $q_5 \varepsilon (-\pi, 0)$

Results

Experiments

In order to collect data to demonstrate the linear relation of the orientation angles and the wrist position, as well as test the proposed method, we conducted experiments with three right-handed subjects (two male and one female). We should note that our goal is to prove this linear relationship works across all subjects and can be applied to estimate the swivel angle of the human arm for anthropomorphic control of the robot arm. A motion capture system with associated positioning markers attached to each rigid link of the human arm were used to compute the joint angles of the shoulder, elbow and wrist. Initially we demonstrated the linear relationship between the angles of the orientation of the upper arm and the forearm and the wrist position using data from a variety of daily tasks and then conducted separate validation tasks with the same human subjects. Six types of experimental tasks were selected from activities of daily living: (Type 1) arm reaching and pointing, (Type 2)placing a water bottle in discrete locations, (Type 3) placing a ping-pong ball in discrete locations, (Type 4) eating, (Type 5) face and head touching and (Type 6) writing. These tasks are chosen from the basic Activities of Daily Life (ADLs) and each task lasts 20 seconds. No initial information of the configuration of the human arm and the robot arm is needed.

Demonstration of the linear relations

Given the elbow and wrist position of the human subjects, we can solve for the actual orientation angles of the upper arm and the forearm. The spherical coordinates of the wrist position can be computed using (5, 6, 7). Therefore, the optimum linear relation is chosen by:

$$\min \int_T^0 (\sigma_{act}(t) - \sigma(t, p_w))dt \quad (27)$$

where T corresponds to 1=5 of total data recording time, $\sigma_{act}(t)$ is the actual angle of the orientation of the upper arm and the forearm, $\sigma(t, P_w)$ is the estimated orientation angle as a linear function of Pw. The combined linear relation between the wrist position and the orientation angles across all tasks and subjects is shown in Figure 5 and the statistical details are given in Table 3. However, due to the arm length difference of the human subjects, the relation will differ from subjects. In Figure 6, two types of graphical analysis are plotted. The mean errors for all the orientation angles are below 5 degrees across all subjects and tasks. It also shows that the mean errors vary from different tasks but are similar $(\pm 1^\circ)$ for different orientation angles.

Method evaluation

I	Orientation angle	Linear function	r^2
1	θ	0.2678R+0.5735ψ+66.46	0.80
2	η	-0.1516R +1.052χ +80.51	0.91
3	α	0.3248R +0.9347χ -154.7	0.95
4	β	0.1471 R-0.981 ψ +24.49	0.95

Table 3: Linear relationship between the intrinsic and extrinsic coordinate.

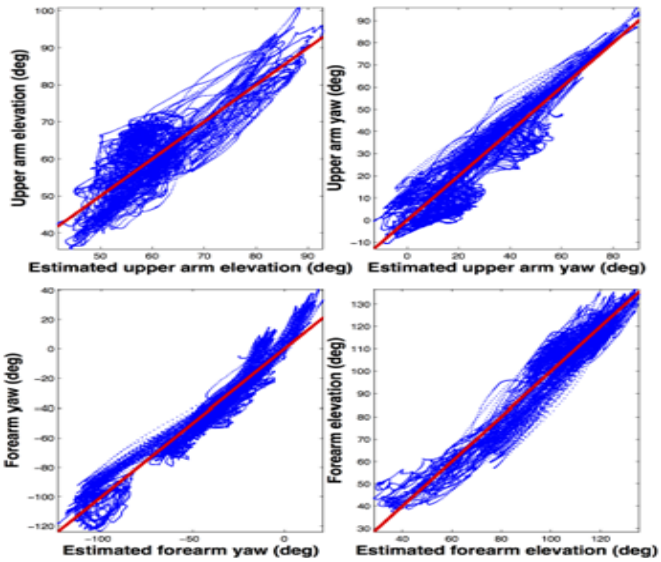

Figure 5: Dependence of intrinsic coordinate on extrinsic parameters across all tasks and subject. The vertical axis represents the actual orientation angles and the horizontal axis represents estimated values from the linear combination of target parameters which gave the best fit to the data.

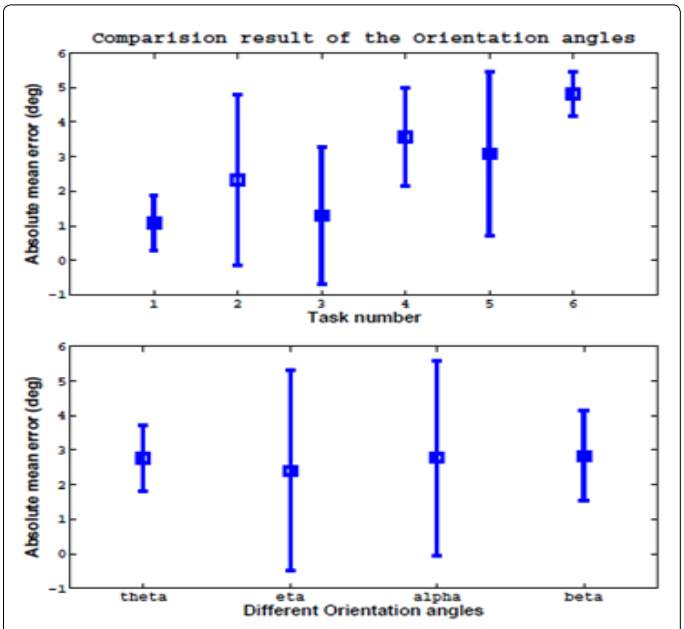

Figure 6: The top plot shows the mean error with associated standard deviation of orientation angles $(\theta, \eta, \alpha, \beta)$ with respect to different types of tasks for all subject. The bottom plot shows the mean error with associated standard deviation with respect to different orientation angles $(\theta, \eta, \alpha, \beta)$

The proposed method was used in order to control a robot arm (LWR4+, KUKA) to reach the desired position and orientation which was identical to that of the human subject during each trial. For the performance estimation, the mean and standard variation of the absolute difference between the the measured swivel angle collected from the subjects during the experiments and the estimated swivel angle of the robot arm based on the proposed criterion were calculated. The performance estimation results are plotted with two representative

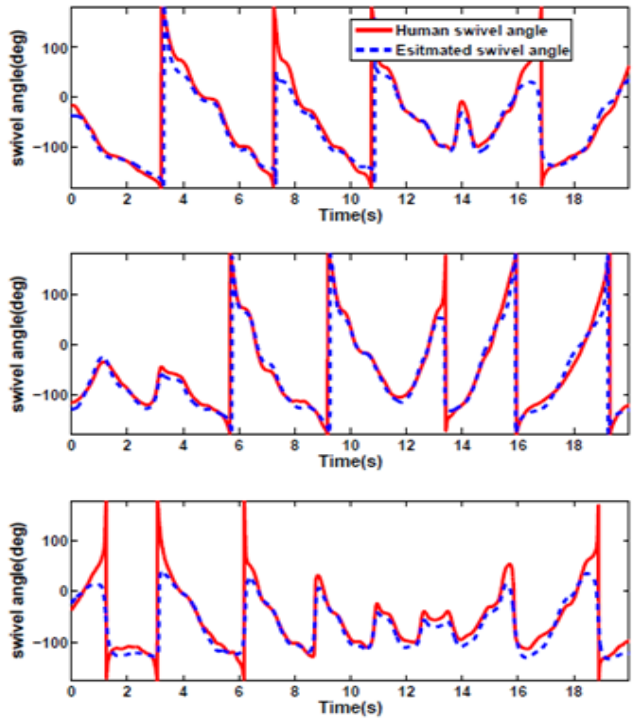

Figure 7: Comparison between the robot (estimated) swivel angle (dotted line) and the human (measured) Swivel angle (solid line) for Type 1 task across all subject. Rows correspond to subject 1,2,3 respectively.

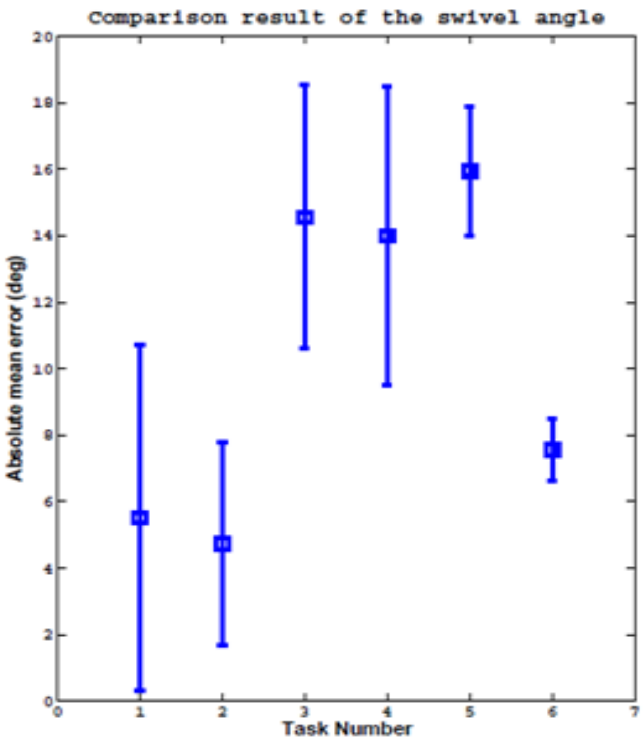

Figure 9: The mean error with associated standard deviation of the swivel angle (ϕ) with respect to types of tasks.

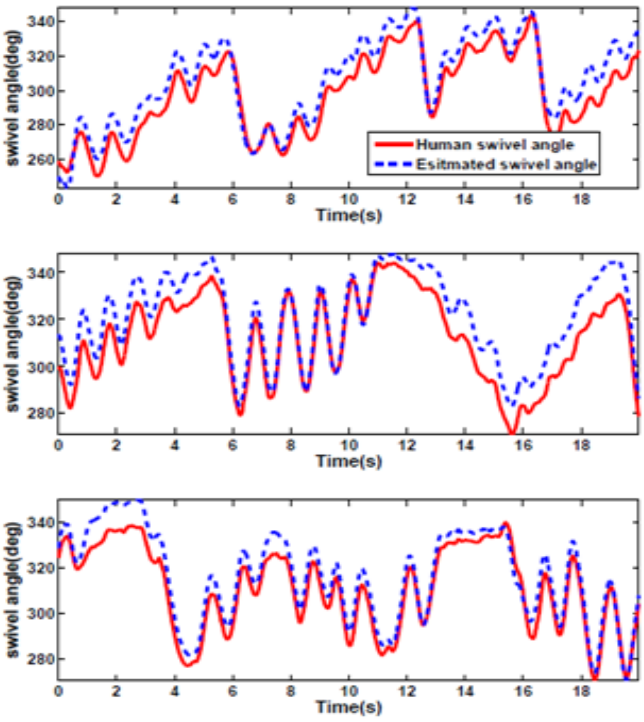

Figure 8: Comparison between the robot (estimated) swivel angle (dotted line) and the human (measured). Swivel angle (solid line) for Type 6 task across all subject. Each row is from subject 1,2,3 respectively.

types of tasks for all subjects. Figures 7 and 8 show the comparison of the human and the robot arm swivel angles for two representative types of tasks. In Figure 9, an analysis of the data indicates that the mean errors vary for different types of tasks. Here we should notice that due to the length difference from the end effector to the wrist, the wrist position of the robot arm will be slightly different from that of the human arm which can cause some error in the estimation of the swivel angle. Also, there is not any initial information for the human arm and the robot arm but the estimation value is still very close to the actual swivel angle with 11° mean error across all tasks and subjects. Comparing the results for Type 2 and Type 3 tasks, it implies that the hand orientation caused by the different types of object has affect on the estimation result (Type 2 task, passing the water bottle has more constraints on the wrist orientation than Type 3 task, passing the ping-pong ball). In order to show that the swivel angle is indeed a possible metric of anthropomorphism, we compared the human and robot arm configurations during the tested tasks. These are shown in Figure 10. It must be noted that the joint angles of the human and robot arm will be different due to the difference in the link lengths of the two. Despite this, the robot arm configurations are very similar to the ones of the human, proving that the swivel angle is representative of anthropomorphism in robot motions.

Conclusions

In this paper we consider the problem of generating human-like motions from the kinematic point of view, taking into account data recorded during a wide variety of everyday life tasks. We use findings from neurophysiology that note the importance of the elbow position and orientation in anthropomorphic arm movements. The

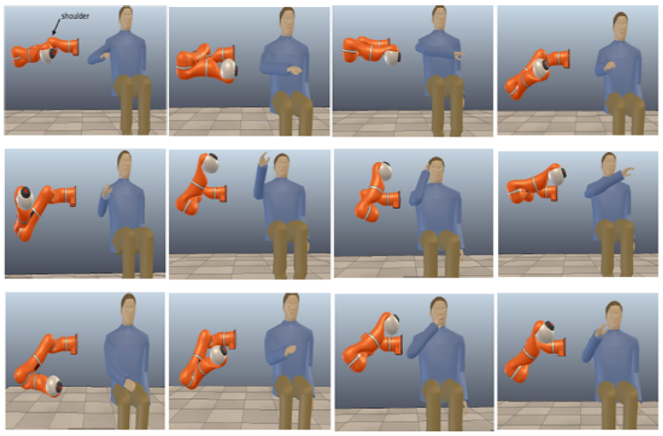

Figure 10: Snapshot of the human arm performing 3D motions and the robot arm driven by the proposed method.

swivel angle of the elbow is used as a human arm motion parameter for the robot arm to mimic. Using experimental data recorded from a human subject during every-day life tasks, we validate the linear relations between intrinsic and extrinsic coordinates that estimates the swivel angle, given the desired end-effector position. Requiring a desired swivel angle simplifies the kinematic redundancy of the robot arm. The proposed method is tested with an anthropomorphic redundant robot arm and the computed motion profiles are compared to the ones of the human subject. We show that the method computes anthropomorphic configurations for the robot arm, even if the robot arm has different link lengths than the human arm, or starts its motion from random configurations. The novelty of the proposed method can be found in two main points. First the method uses the concept that the positioning of the elbow joint is a decisive factor of anthropomorphic configurations in humans. Based on that, we define the swivel angle and design our inverse kinematic problem in order to provide similar (but not identical) robot swivel angles with those of the human during every-day life tasks. This results to an analytic closed-form solution of the inverse kinematic problem. Secondly, the method is generalizable, since it can be used in a wide variety of redundant robot arms, as long as an elbow-equivalent point is defined on the robot arm.

References

1. Edsinger A, Kemp CC (2007) Human-Robot Interaction for Cooperative Manipulation: Handing Objects to One Another. The 16th IEEE International Symposium on Robot and Human interactive Communication.
2. Asfour T, Dillmann R (2003) Human-like motion of a humanoid robot arm based on a closed-form solution of the inverse kinematics problem. Intelligent Robots and Systems 2:1407-1412.
3. Veljko P, Spyros T, Dragan K, Goran D (2001) Human-like behavior of robot arms: general considerations and the handwriting task—Part I: mathematical description of human-like motion: distributed positioning and virtual fatigue. Robotics and Computer-Integrated Manufacturing 17:305-315 .
4. Hyunchul K, Miller LM, Byl N, Abrams G, Rosen J (2012) Redundancy Resolution of the Human Arm and an Upper Limb Exoskeleton. Biomedical Engineering 59: 1770-1779.
5. Hyunchul K, Miller LM, Rosen J (2011) Redundancy and joint limits of a seven degree of freedom upper limb exoskeleton. Annual International Conference of the IEEE on Engineering in Medicine and Biology Society, Boston.
6. Hyunchul K, Miller LM, Al-Refai A, Brand M, Rosen J (2011) Redundancy resolution of a human arm for controlling a seven DOF wearable robotic system. Annual International Conference of the IEEE on Engineering in Medicine and Biology Society, Boston.
7. Cruse H, Wischmeyer E, Brüwer M, Brockfeld P, Dress A (1990) On the cost functions for the control of the human arm movement. Biological Cybernetics 62: 519-528.
8. Hollerbach JM, Ki Suh (1987) Redundancy resolution of manipulators through torque optimization. Robotics and Automation 3:308-316.
9. Khatib O, Burdick J (1986) Motion and force control of robot manipulators. Robotics and Automation 3:1381-1386.
10. Hogan H (1984) An organizing principle for a class of voluntary movements. The Journal of Neuroscience 4: 2745-2754.
11. Sief NA, Winters J(1989) Changes in musculoskeletal control strategies with loading: inertial,.isotonic, random. in ASME Biomech. Symp, pp. 355{358, 1989.
12. Temprado JJ, Swinnenb SP, Carsonc RG, Tourmenta A, Laurenta M (2003) Interaction of directional, neuromuscular and egocentric constraints on the stability of preferred bimanual coordination patterns. Human Movement Science 22:339-363.
13. Debaerea F, Wenderotha N, Sunaertb S, Van Heckeb P, Swinnen SP (2004) Cerebellar and premotor function in bimanual coordination: parametric neural responses to spatiotemporal complexity and cycling frequency. NeuroImage 21: 1416-1427.
14. Latash ML (1993) Control of human movement.
15. Potkonjak V, Kostic D, Tzafestas S, Popovic M, Lazarevic M, Djordjevic G (2001) Human-like behavior of robot arms: general considerations and the handwriting task part ii: the robot arm in handwriting. Robotics and Computer-Integrated Manufacturing 17: 317- 327.
16. Ude A, Man C, Riley M, Atkeson CG (2000) Automatic generation of kinematic models for the conversion of human motion capture data into humanoid robot motion.
17. Kim C, Kim D, Oh Y (2005) Solving an inverse kinematics problem for a humanoid robot2019s imitation of human motions using optimization," in ICINCO'05, pp. 85{92, 2005.
18. Pollard N, Hodgins JK, Riley M, Atkeson C(2002) Adapting human motion for the control of a humanoid robot .IEEE International Conference on Robotics and Automation 2: 1390-1397.
19. Caggiano V, De Santis A,Siciliano B, Chianese A (2006) A biomimetic approach to mobility distribution for a human-like redundant arm. The First IEEE/RAS-EMBS International Conference on Biomedical Robotics and Biomechatronics.
20. Artemiadis P, Katsiaris P, Kyriakopoulos K (2010) A biomimetic approach to inverse kinematics for a redundant robot arm. Autonomous Robots 29: 293-308.
21. Korein JU (1986) A geometric investigation of reach.
22. Sciavicco L, Siciliano B(1996) Modeling and control of robot manipulators.
23. Tolani D, Goswami A, Badler NI(2000) Real-time inverse kinematics techniques for anthropomorphic limbs. Graphical Models 62: 353- 388.
24. Soechting JF, Flanders M (1989) Sensorimotor representations for pointing to targets in three dimensional space. Journal of Neurophysiology 62: 582-594.
25. Soechting JF, Flanders M (1989) Errors in pointing are due to approximations in sensorimotor transformations. Journal of Neurophysiology 62: 595-608.